EE137 Final Presentation:

LIDAR

Grant Beatty - Nathaniel Sicard

What is LIDAR?

- Generally accepted as an acronym for ‘laser imaging, detection, and ranging or a combination of the words ‘light’ and ‘radar.’
- Method for to detecting the return times of laser pulses, which can be extrapolated into distance measurements.
- Used in the creation of three dimensional images, which have a wide variety of uses.

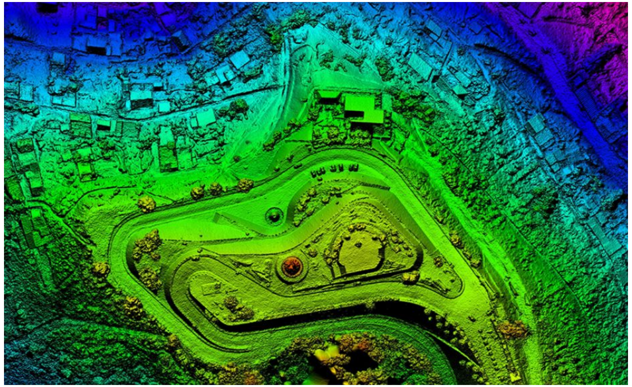

History of LIDAR

- Hughes Aircraft Company developed the first lidar system in 1961, following the invention of the laser
- Intended to assist in tracking satellites
- Currently has applications in geological surveying, position and navigation systems, archeological maps, and velocity detection used by law enforcement

How it Works

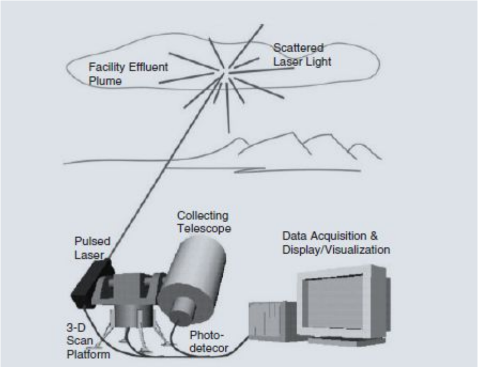

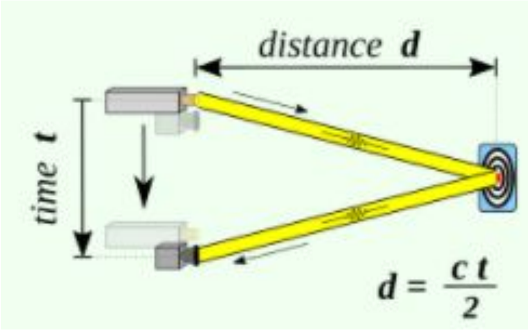

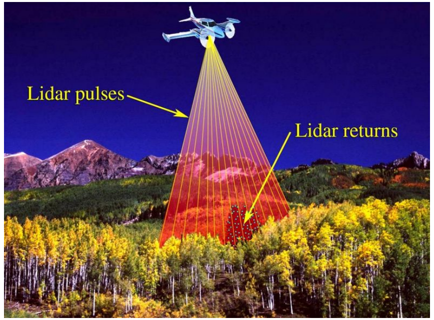

- Pulses of laser light are beamed from the Lidar system into an environment
- Return times from the pulses of light are used to calculate distances to the surface
- The measured distances are used to produce a high resolution digital elevation model, DEM
- Doppler shifts can be detected to determine object speed or wind speed

How it Works

- The system involves a laser transmitter, filter, photodetector, and a computational system for mapping and analyzing the data
- The signals from the detectors are measured by a transient digitizer which samples voltage signals at equal time intervals and creates the corresponding digital signals. This data is stored in memory for further analysis and displayed.

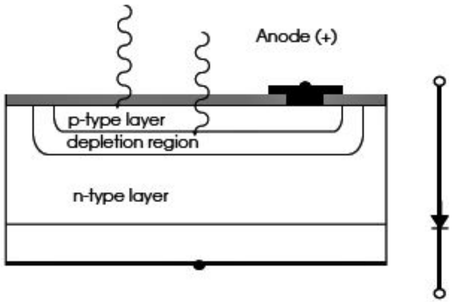

Fig. 4.1. A cross section of a typical silicon photodiode.

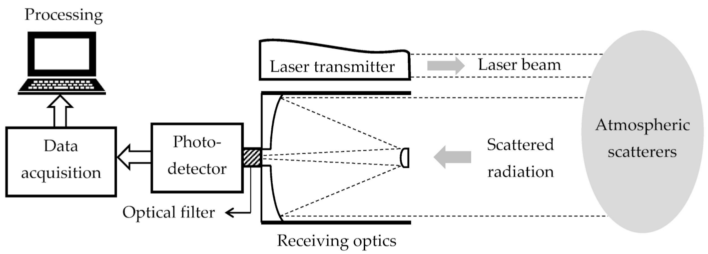

Notable Applications

Self-driving cars

Agriculture

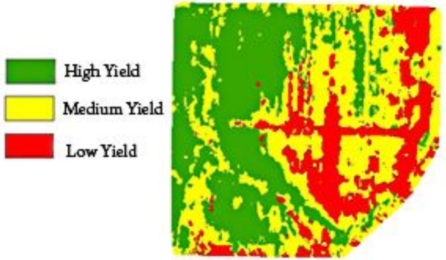

Oceanography

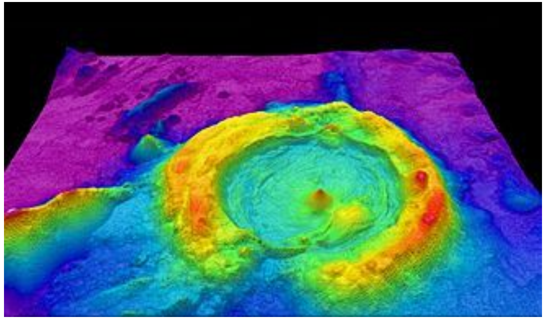

Archaeology

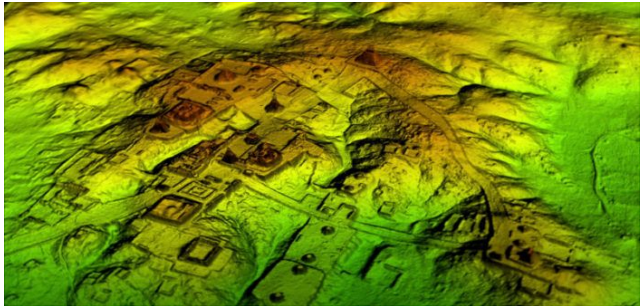

Atmospheric Lidar

Meteorological applications

- Wind speed
- Cloud measurements
- Particle Profiles
- Temperature

Lidar Types

- **Elastic Lidar**
- DIAL Lidar
- Rayleigh Lidar
- Mie Lidar
- Raman Lidar

The Physics of Atmospheric Lidar

Rayleigh Scattering

- Laser light is elastically scattered by molecules smaller than the wavelength of the radiation. Rayleigh scattering is due to the electric polarizability of particles. The oscillating electric field of a light wave causes particles in the air to become small radiating dipoles that emit light. Most photons in the air are elastically scattered.

$$I = I_0 \frac{1+\cos^2\theta}{2R^2}\left(\frac{2\pi}{\lambda}\right)^4\left(\frac{n^2-1}{n^2+2}\right)^2\left(\frac{d}{2}\right)^6$$

I:intensity of light scattered
I_o:intensity(initial)
n:refractive index
R:distance to particle
θ:scattering angle
λ:wavelength
d:particle diameter
σ: cross-section

Averaging this over all angles gives the Rayleigh scattering cross-section

$$\sigma_s = \frac{2\pi^5}{3}\frac{d^6}{\lambda^4}\left(\frac{n^2-1}{n^2+2}\right)^2$$

(particles per unit volume)×(the cross-section σ_s)=(fraction of light scattered per unit length)

The Physics of Atmospheric Lidar

Mie Scattering

- Mie scattering describes the scattering of light waves by a homogeneous sphere. It acts on particles more comparable to the size of of the light wavelength such as water droplets in clouds, moisture, dust, pollen, and smoke. Like Rayleigh scattering it is also elastic.

Qe: extinction coefficient
Qs: scattering coefficient
Qa: absorption coefficient
σ: cross section
n: refractive index
a: particle radius
k:2π/λ

$$Q_e = Q_s + Q_a$$

$$Q_s = \frac{2}{k^2 a^2} \sum_{n=1}^{\infty} (2n+1)(|a_n|^2 + |b_n|^2)$$

$$Q_e = \frac{2}{k^2 a^2} \sum_{n=1}^{\infty} (2n+1)\Re(a_n + b_n)$$

$$\sigma_e = \sigma_s + \sigma_a \text{ and } Q_e = Q_s + Q_a$$

$$Q_i = \frac{\sigma_i}{\pi a^2}$$

(particles per unit volume)×(the cross-section σ)=(fraction of light scattered per unit length)

The Physics of Atmospheric Lidar

Raman Scattering

- Raman scattering happens when a laser photon excites a molecule to a virtual electronic energy level. The molecule's electronic energy level drops back down and light is emitted. Raman scattering is inelastic so the wavelength of the returning light is changed. Each molecule has a signature Raman scattering.

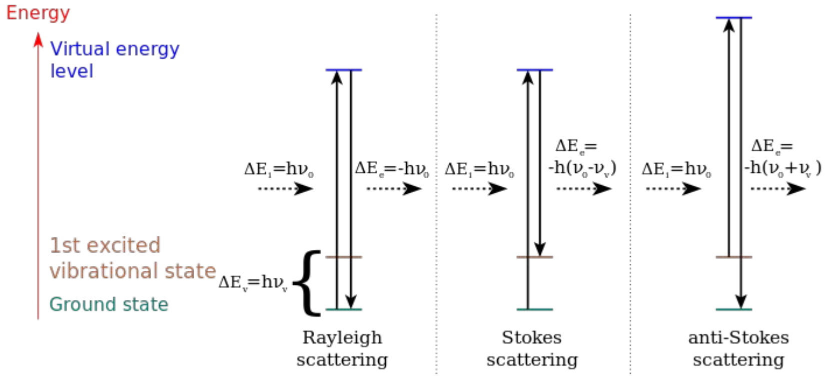

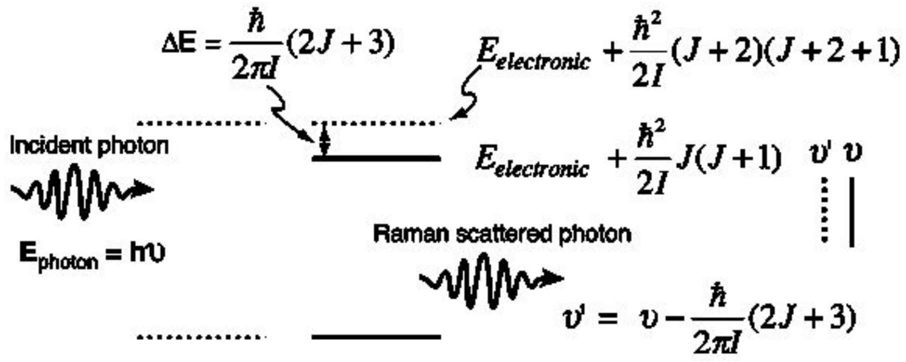

Atmospheric Lidar Scans

Vertical Dial Scan

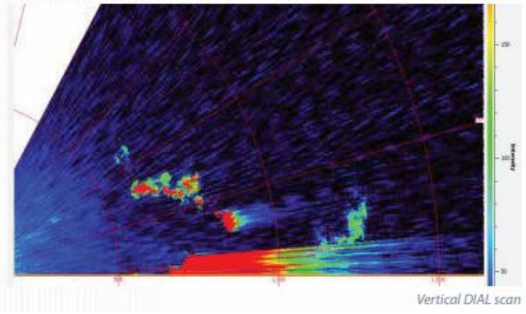

RHI Scan

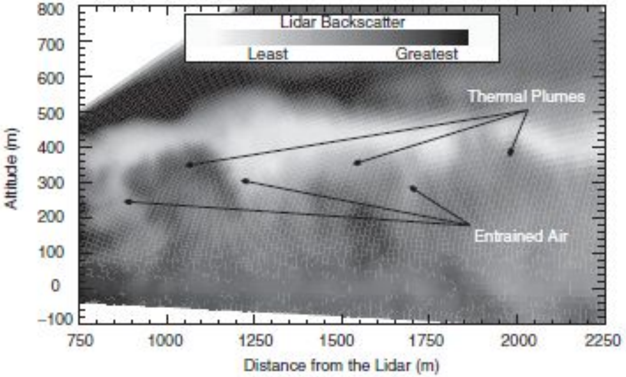

Time Scan

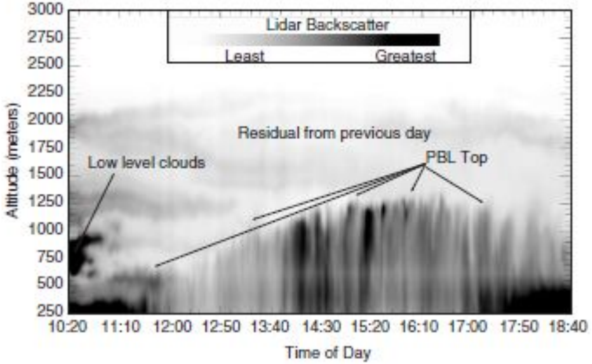

PPI Scan

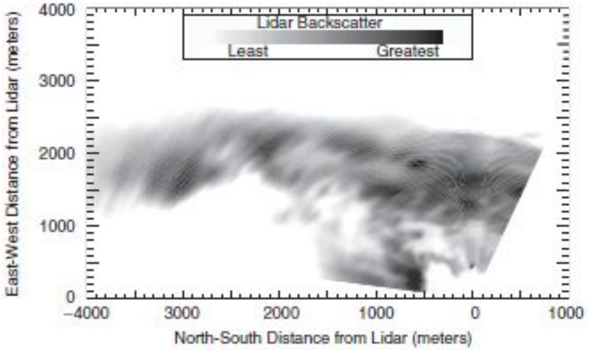

Implementation of Atmospheric Lidar

Block diagram with the most significant components

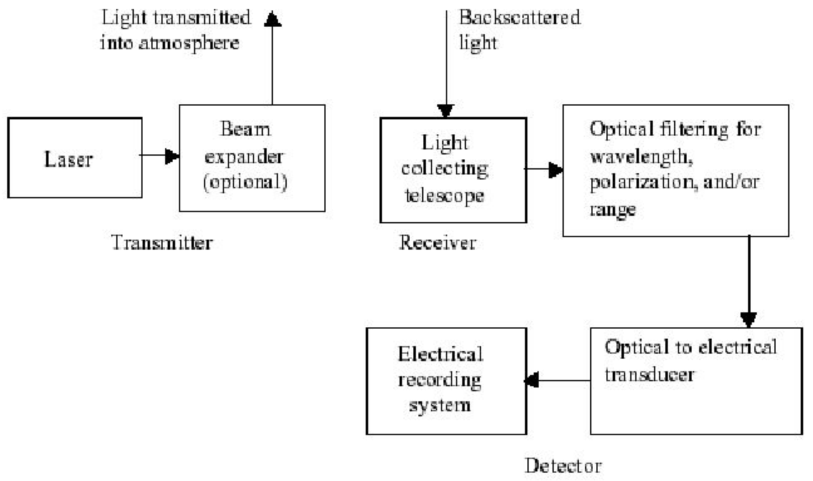

Atmospheric Lidar

Limiting Factors

- Eye Safety
- Weak signal from backscattered light
- (SNR) Signal to Noise Ratio
- Filtering
- Large or expensive Equipment
- Range Resolution
- Power Consumption

Atmospheric Lidar

Eye Safety

- In the United States, the accepted document that regulates laser eye safety issues is the American National Standard for the Safe Use of Lasers
- Eyesafe wavelengths: (λ<400 nm), (λ>1,400 nm)
- The typical Lidar uses the range, 350-1064 nm

TABLE 3.2. Maximum Permissible Exposure (MPE)

Wavelength (μm)	Exposure Duration, t (s)	Maximum Permissible Exposure (J/cm²)
0.180–0.302	10^{-9}–3×10^{4}	3×10^{-3}
0.303	10^{-9}–3×10^{4}	4×10^{-3}
0.304	10^{-9}–3×10^{4}	6×10^{-3}
0.305	10^{-9}–3×10^{4}	10^{-2}
0.306	10^{-9}–3×10^{4}	1.6×10^{-3}
0.307	10^{-9}–3×10^{4}	2.5×10^{-2}
0.308	10^{-9}–3×10^{4}	4×10^{-2}
0.309	10^{-9}–3×10^{4}	6.3×10^{-2}
0.310	10^{-9}–3×10^{4}	0.1
0.311	10^{-9}–3×10^{4}	0.16
0.312	10^{-9}–3×10^{4}	0.25
0.313	10^{-9}–3×10^{4}	0.40
0.314	10^{-9}–3×10^{4}	0.63
0.315–0.400	10^{-9}–10	$0.56\,t^{1/4}$
0.400–0.700	10^{-9}–1.8×10^{-5}	5×10^{-7}
0.700–1.050	10^{-9}–1.8×10^{-5}	$5 \times 10^{-7} * 10^{2(\lambda-0.700)}$
1.050–1.400	10^{-9}–5.0×10^{-5}	$5 * C_c \times 10^{-6}$
1.400–1.500	10^{-9}–10^{-3}	0.1
1.500–1.800	10^{-9}–10	1.0
1.800–2.600	10^{-9}–10^{-3}	0.1
2.600–10^{3}	10^{-9}–10^{-7}	10^{-2}

Atmospheric Lidar

Eye Safety Challenges

Long Wavelength: (λ>1,400 nm)

- Molecular scattering is reduced while larger particle scattering is increased
- Rayleigh scattering is proportional to (1/λ)^4
- Thermal noise when detecting infrared light
- Solid-state detectors for this wavelength are more expensive.

Short wavelength: (λ<400 nm)

- The scattering at this wavelength is mostly molecular.
- Mie scattering is proportional to (λ)^2
- Ultraviolet light scattered around the lidar system

The typical Lidar uses the range, 350-1064 nm

Atmospheric Lidar

Equipment Size

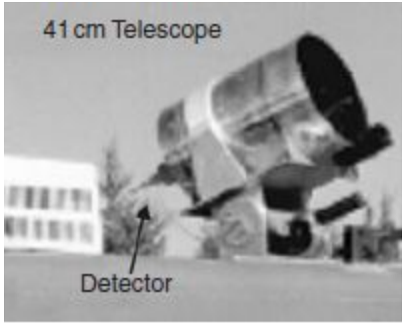

Micropulse Lidar System

523 nm MPL
- Max range: 18 km
- Range resolution 30-300m
- SNR: 50-100
- Dimensions: 300 x 350 x 850 mm
- Weight: 27 kg

Components
- Nd:YLF laser
- ~25 mW pulse
- Schmidt-Cassegrain telescope
- narrow band interference filter (3nm width)
- photon-counting avalanche photodiodes
- Computer

*Nd:YLF laser (Neodymium-doped Yttrium Lithium Fluoride)

Laser-Telescope Overlap

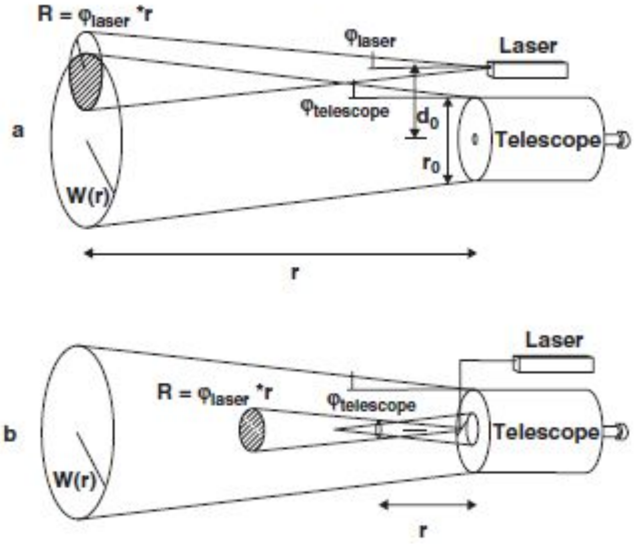

Scheimpflug principle

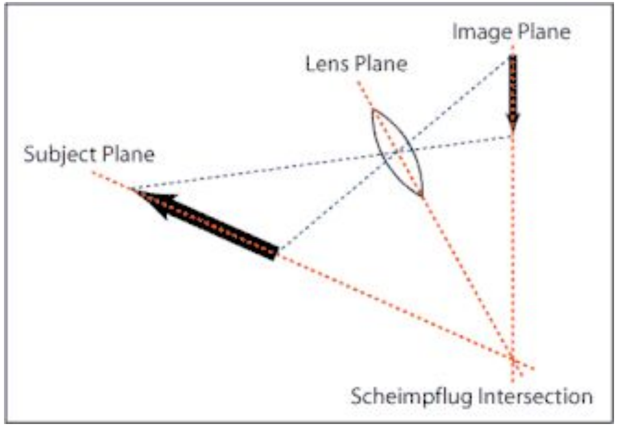

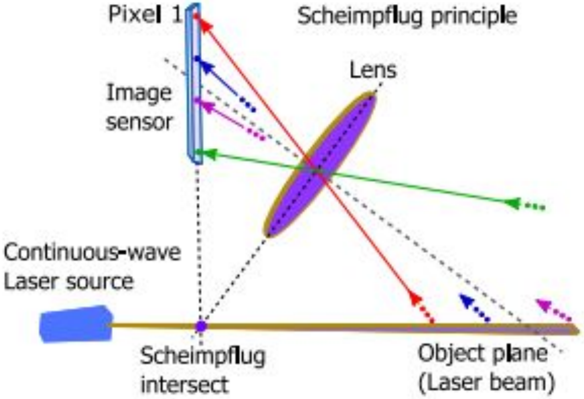

Scheimpflug Lidar

808 nm mini-Scheimpflug lidar

- Max Range: 7-10 km
- Range resolution at 2 km is 80m
- SNR averages to 100 at night and 200
- Dimensions:690mm×540mm×200mm
- Weight: 20 kg

Components

- 4 W high-power laser diode (inexpensive)
- ~120 mW pulse
- Newtonian telescope
- narrow band interference filter (3nm width)
- CMOS image sensor (2048×1024 pixels)(inexpensive)
- Computer

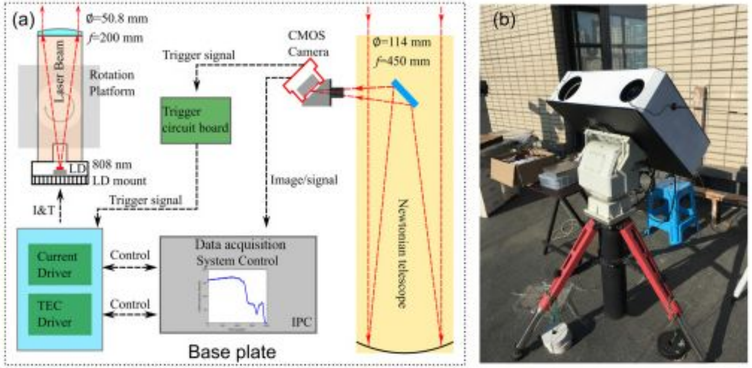

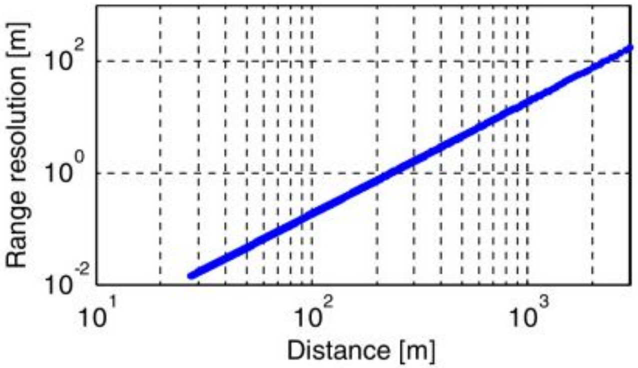

Future Development

Purple Crow Lidar (PCL) system
located in London, Ontario, Canada

Nitrogen channel		
Scan type	Precision	Recall
Cloud	0.94	0.91
Clear	0.96	0.98
Bad	1.00	1.00
LR channel		
Scan type	Precision	Recall
Clear	0.99	0.99
Bad	0.96	0.95
HR channel		
Scan type	Precision	Recall
Clear	0.98	1.00
Bad	0.98	0.94

Machine Learning and
Image Processing

- 4,500 profiles from the LR, HR, and the nitrogen vibrational Raman channels
- 70 % of the data was used to train the algorithms
- 30% was tested by the algorithms

Nitrogen HR LR

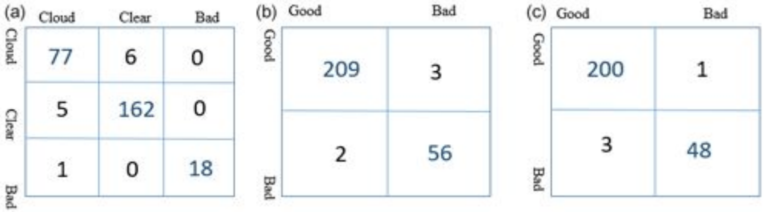

Airborne Lidar

General idea

- Utilizes aircraft
- GPS used to calculate aircraft position
- Pulses sent out and return data is used to compute DEM

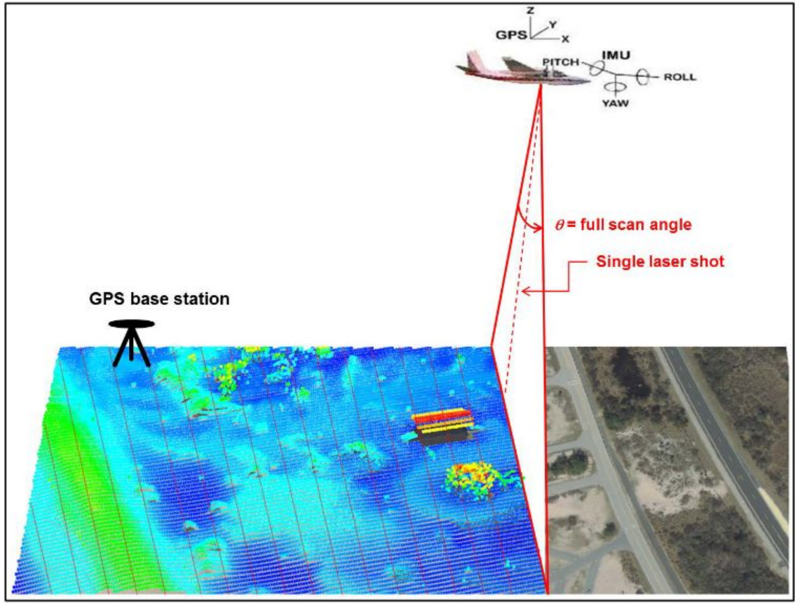

Figure 2-1. Schematic diagram of airborne lidar performing line scanning resulting in parallel lines of measured points (other scan patterns exist, but this one is fairly common)

Airborne Lidar
Block Diagram

- block diagram of ALS
- position and movement of aircraft
- Global positioning system
- Range data
- GIS and CAD software
- Processing system

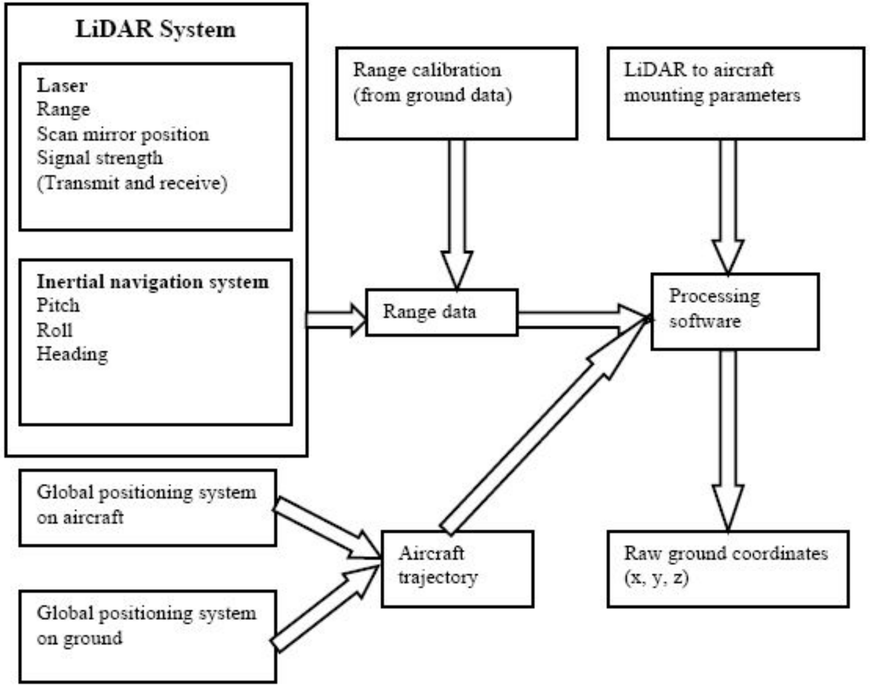

Airborne Lidar

Shortcomings

- Expensive/heavy material on disposable drones
- Difficulty obtaining bathymetric data (weight, power constraints)
- Inadequate long range small target detection

Airborne Lidar

Improvements in technology

- Factors associated with improving Lidar technology:
    - high accuracy and resolution over given range
    - high signal to noise ratio
    - less power consumption
    - greater data processing
    - weight efficiency

- Continued Development in these technologies:
    - Sensitive electromagnetic detecting instruments
    - Powerful laser transmitters
    - Faster and more powerful computers
    - Capable aircraft

- There is a limit to how sensitive, powerful, and big typical components can be

Airborne Lidar

Signal to noise ratio

- Electromagnetic radiation is common in atmosphere
- Signals from random sources have random properties and can corrupt distancing data
- High SNR corresponds to higher resolution images and more confidence DEM accuracy

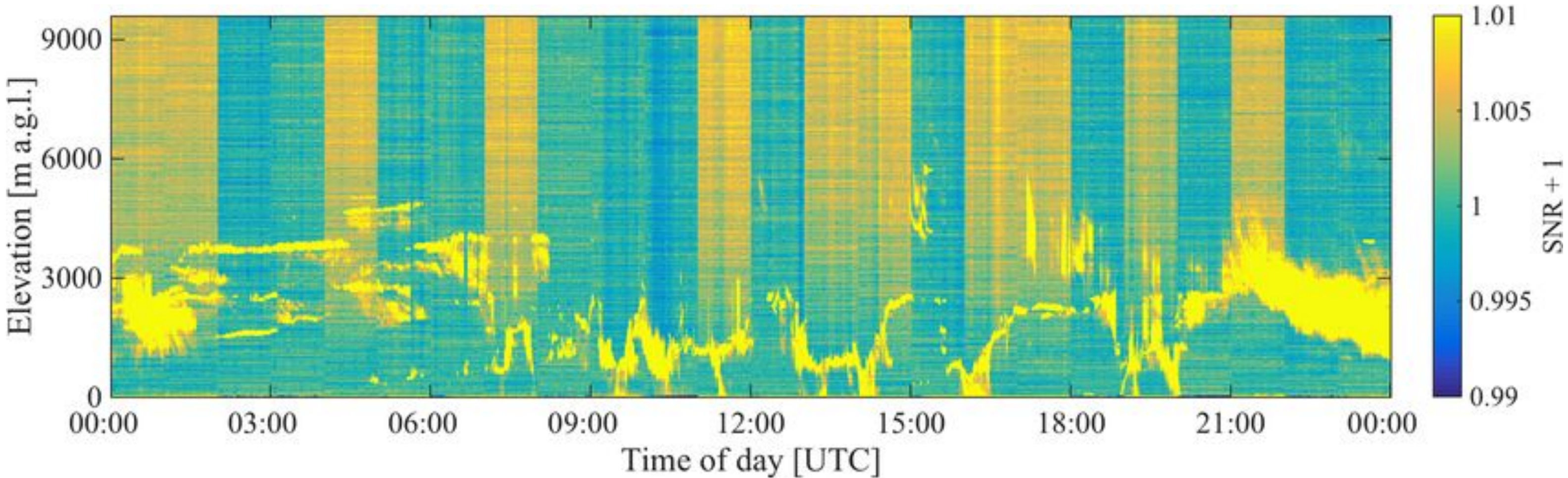

Airborne Lidar

ALSM

- Typical system: Airborne laser swath mapping
- Laser pulse energies > 100 microjoules
- High SNR
- Favor simplified detection
- Power limited by weight

Coutesy of the School of Mechanical and Precision Instrument Engineering, Xi'an University of Technology, Xi'an 710048, China

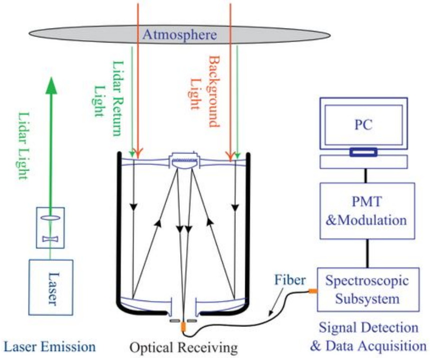

Fig. 1. Schematic diagram of the Lidar system.

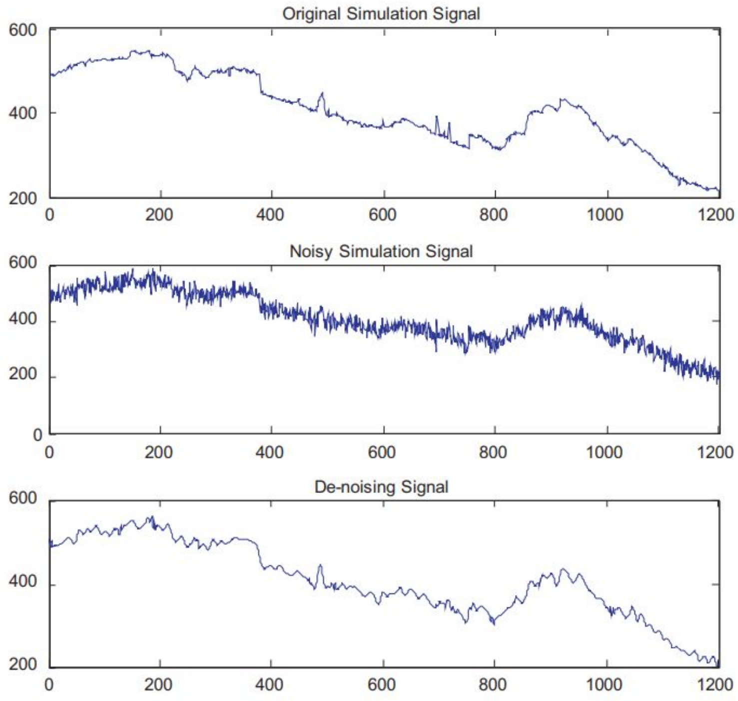

Fig. 4. Simulation of de-noising algorithm.

Airborne Lidar
Single photon detectors

- Pros:
  - Rising interest in single photon detection
  - Higher performance
  - Easier to use
- Cons:
  - Reduced SNR
- Types:
  - Silicon photomultiplier (SiPM)
  - superconducting nanowire single-photon detector (SNSPD)
- Employs Single Photon Avalanche Diodes (SPADs)

Airborne Lidar

SPAD

- Single-photon avalanche diode
- High reverse bias
- Can create ‘Avalanche’ current from single photon
- Photons can be counted!
- Incident photon return time can be counted!

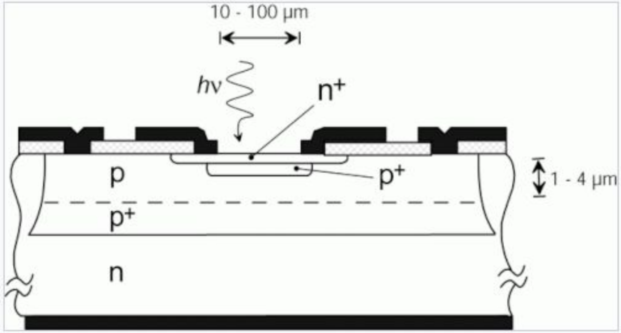

Figure 1 - Thin SPAD cross-section.

Commercial single-photon avalanche diode module for optical photons

Airborne Lidar
SiPM

- Silicon photomultipliers
- Solid state photon detector
- Single photon avalanche detector diodes

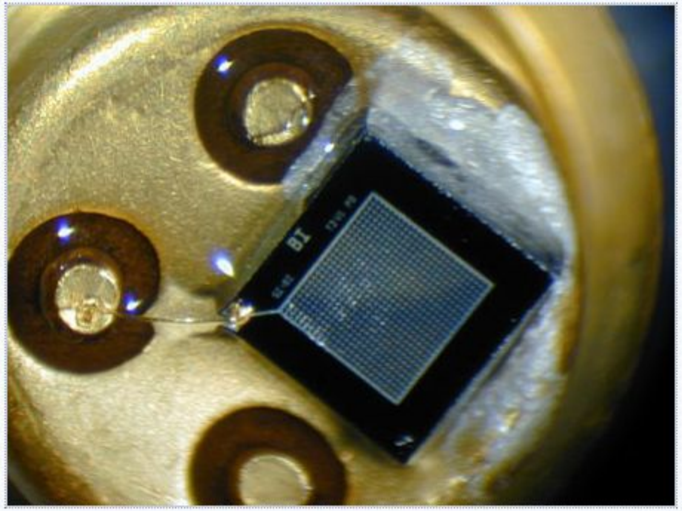

One of the first SiPM produced by FBK research center (formerly IRST) located in Trento, Italy.

Airborne Lidar

SNSPD

- superconducting nanowire single-photon detectors (SNSPD)
- Historically NbN or NbTiN, with single-photon response to UV near-infrared
- Timing jitter around 30–100 ps (very fast!)
- Very expensive!!

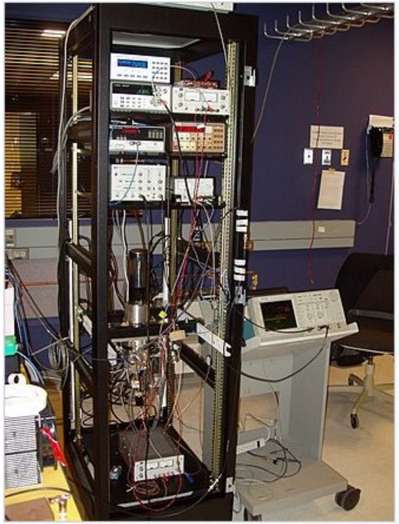

Superconducting nanowire single-photon detector in the DARPA Quantum Network laboratory at BBN, June 2005

Airborne Lidar

LSNR

- Reduced laser energies (<10 microjoules)
- Reduced frequency
- Reduced SNR
- Careful consideration to instrument design
- expensive!

Courtesy of University of Florida Department of Civil & Coastal Engineering

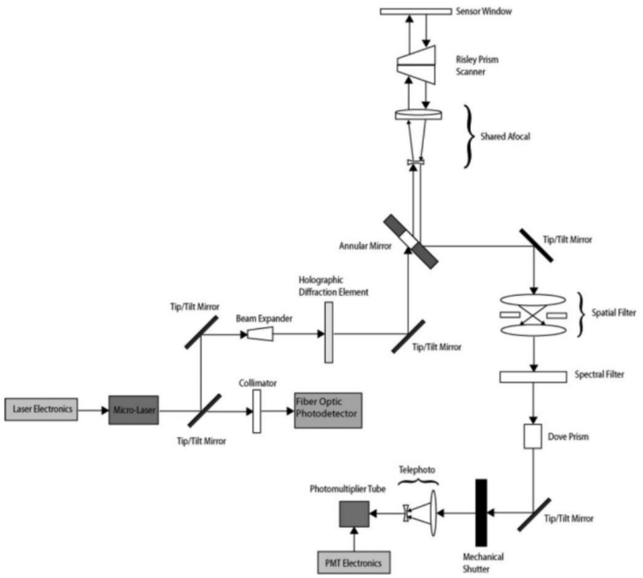

Fig. 1. Detailed optical path with turning mirrors, mechanical shutter, receiver electronics, and fiber optic detector.

Airborne Lidar

CATS

- Coastal Area Tactical-mapping System
- Uses Nd:YAG at 532 nm
- Cycling pulse of 8kHz
- 10x10 multi-channel PMT

Courtesy of University of Florida Department of Civil & Coastal Engineering

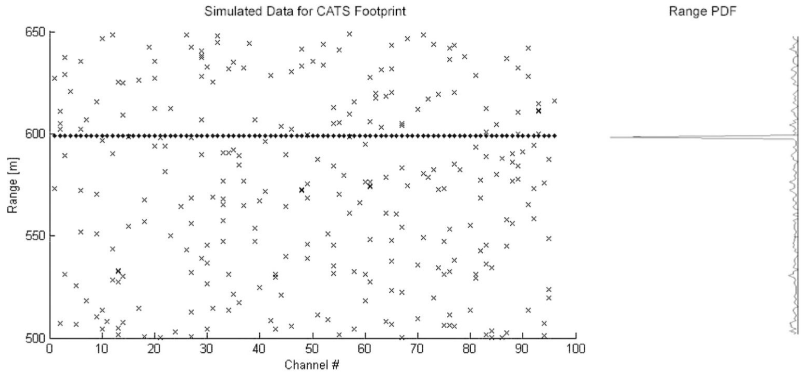

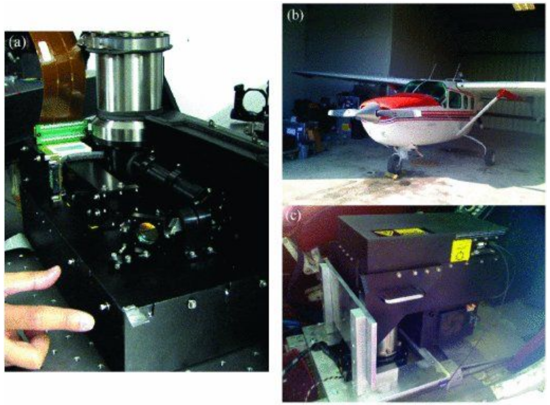

Fig. 1. Single realization for one CATS footprint (96 channels), simulated over a flat level surface. Signal events are plotted as dots and noise events appear as "x"s. The distribution of ranges across the range gate is shown on the right. A lidar altitude of 600 m was specified, and solar zenith angle was set to 0 degrees from earth normal to simulate high noise levels. Range gate specifications include the onset value (500 m in this case) and duration (150 m).

Airborne Lidar

CATS - ALB LSNR

- Airborne laser bathymetry
- Removed dependency on red and infrared spectrum
- Focus on green band
- No need for eye safety measures due to low power
- Lidar Link equation: Poisson distribution (right) details relationship between generated and transmitted PE
- Expression(s) for laser energy (left)

Kristofer Y. Shrestha, Member, IEEE, William E. Carter,
K. Clint Slatton, Senior Member, IEEE, and Tristan K. Cossio, Member, IEEE

$$E_{t,topo} = \frac{hv \cdot n_s}{n_h n_q n_r \cdot \rho_\lambda \cdot \cos(\alpha) \cdot \frac{A_r}{\pi R^2} \left[\exp(-\beta_{e\lambda} R)\right]^2}$$

$$E_{t,bathy} = \frac{hv \cdot n_s}{n_h n_q n_r \cdot \rho_\lambda \cdot \cos(\alpha_t) \cdot \frac{A_r}{\pi (R_{air}+R_w)^2}} \cdot \frac{1}{[1 - r_{\text{int}}(\alpha_s)]^2 \cdot [\exp(-\beta_{e\lambda} R_{air})]^2 \cdot [\exp(-c_\lambda R_w)]^2}$$

$$P(n_t, n_s) = n_s^{n_t} \cdot \frac{e^{-n_s}}{n_t!}$$

TABLE I
SAMPLE SYSTEM PARAMETERS FOR LIDAR LINK EQUATIONS

n_h	0.8
n_q	0.28
n_r	0.4
h	$6.63 \cdot 10^{-34}$ J·s
v	$5.64 \cdot 10^{14}$ Hz
ρ_λ	0.15
a	5°
A_r	$3.3 \cdot 10^{-3}$ m^2
$B_{e,\lambda}$	$0.297 \cdot 10^{-3}$ m^{-1}
R	600 m
a_t	3.5°
R_{air}	600 m
R_w	5 m
a_s	5°
a_r	3.76°
r_{int}	0.01
$a_{\lambda,pure}$	0.0517 m^{-1}
$b_{\lambda,pure}$	0.0025 m^{-1}
$a_{\lambda,coastal}$	0.1790 m^{-1}
$b_{\lambda,coastal}$	0.2190 m^{-1}

Airborne Lidar

CATS - ALB LSNR(results)

Kristofer Y. Shrestha, Member, IEEE, William E. Carter,
K. Clint Slatton, Senior Member, IEEE, and Tristan K. Cossio, Member, IEEE

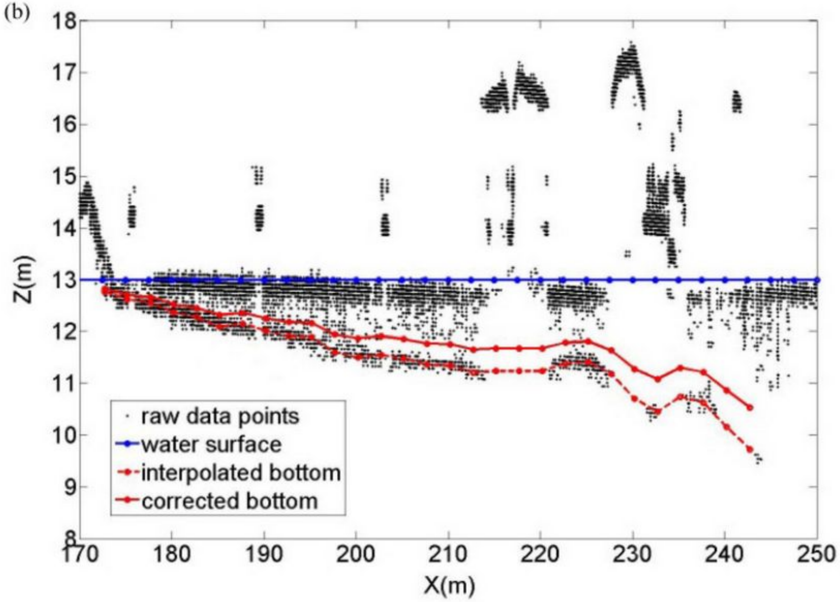

Fig. 17. Flight testing in St. Augustine, FL, over docks on the Intracoastal Waterway. A slight roll of the aircraft is most likely present, causing the interrogated profile to be displaced approximately 1 m to the left of the red flight line in the aerial photo. (a) Aerial photograph near boat docks and shallow launch region with a flight line. (b) Off-nadir profile, single channel (18), 2500 V, all returns, with the processed data depicting saltwater penetration out to 2.5 m. Note the compression of the x-axis (necessary to depict the entire range of bottom sensing).

Airborne Lidar

Small Target Detection

- Single photon avalanche diode (SPAD) using InGaAs/InP
- erbium-doped fiber laser operating at a wavelength of 1550 nm
- 800 ps duration pulses at 125kHz
- Although not within LSNR specs, experimentally justifies key concept!

Institute of Photonics and Quantum Sciences, School of Engineering and Physical Sciences, Heriot-Watt University, Edinburgh

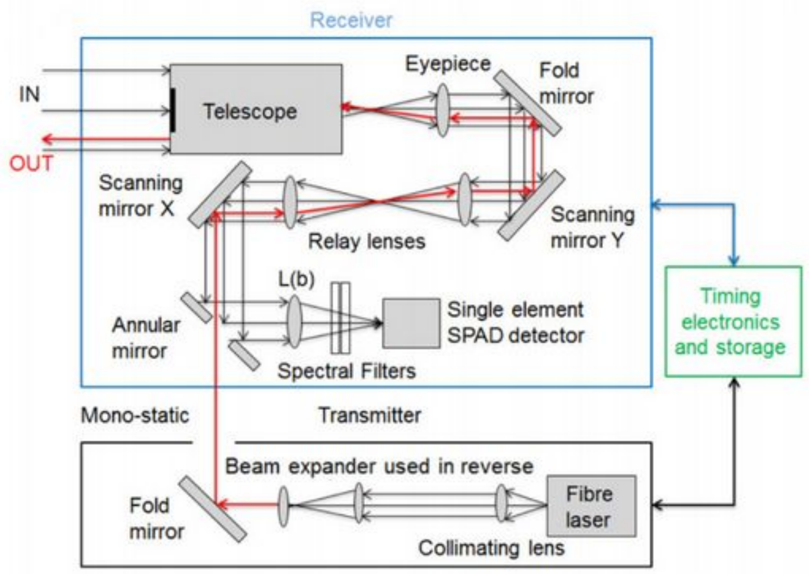

Fig. 1. Schematic diagram of the experimental setup of the system operating in a mono-static configuration with a scanned single-element SPAD detector.

Airborne Lidar
Small Target Detection(results)

- Several objects tested
- Robust 3D images created
- Acquisition times reduced by factor of 10
- Single photon per pixel

Institute of Photonics and Quantum Sciences, School of Engineering and Physical Sciences, Heriot-Watt University, Edinburgh

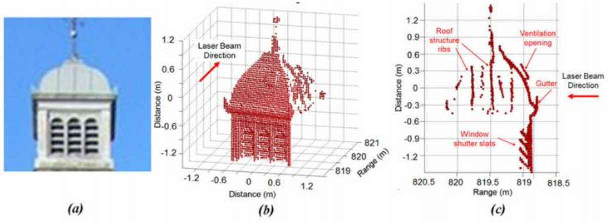

Fig. 2. (a) A two-dimensional visible-band image of the top of the clock tower acquired with a camera lens of f = 200 mm. (b) Depth plot of the top of the clock tower at a range of ~800 m with 85 × 85 scan points and an acquisition time of 170 ms per pixel. (c) Depth plot of the top of the clock tower at a range of ~800 m with 85 × 85 scan points and an acquisition time of 170 ms per pixel showing side view of the target.

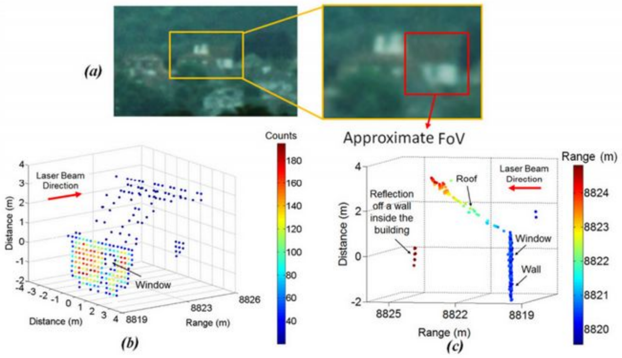

Fig. 3. (a) Visible-band image of a residential building taken with an f = 200 mm camera lens. (b) Depth - intensity plot of the building imaged with 32 × 32 scan points over a range of ~8.8 km. (c) Depth plot of the building imaged with 32 × 32 scan points over a range of ~8.8 km; side view of the target.

Airborne Lidar

Conclusion

- Single photon detectors solve many issues w/r/t Airborne lidar (and other technology!)
  - Airborne lidar limited by weight, power, component cost
  - PMTs based on SPAD technology
  - No classic anaolg, must use quantum mechanics
  - LSNR (CATS, topographic DEM, bathymetric DEM)
  - Small target detection

Different detectors for applications other than lidar

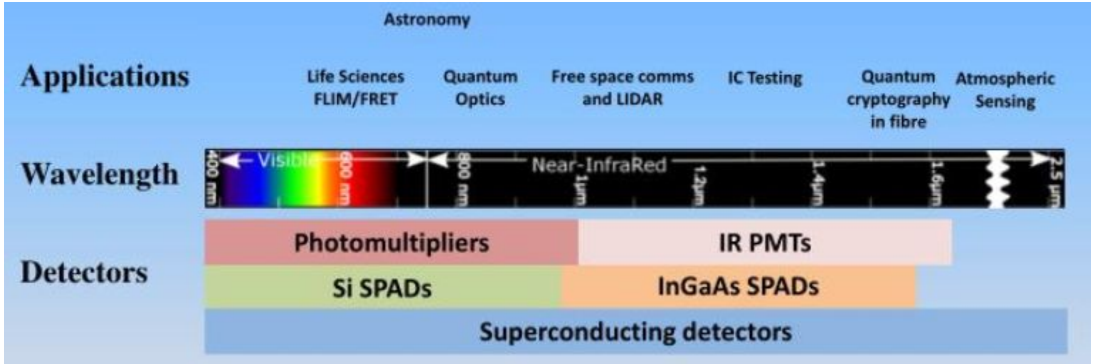

Atmospheric Lidar

Conclusion

- Meteorological and environmental applications
- Uses Rayleigh, Mie and Raman scattering
- More compact and inexpensive designs
- Machine learning applications

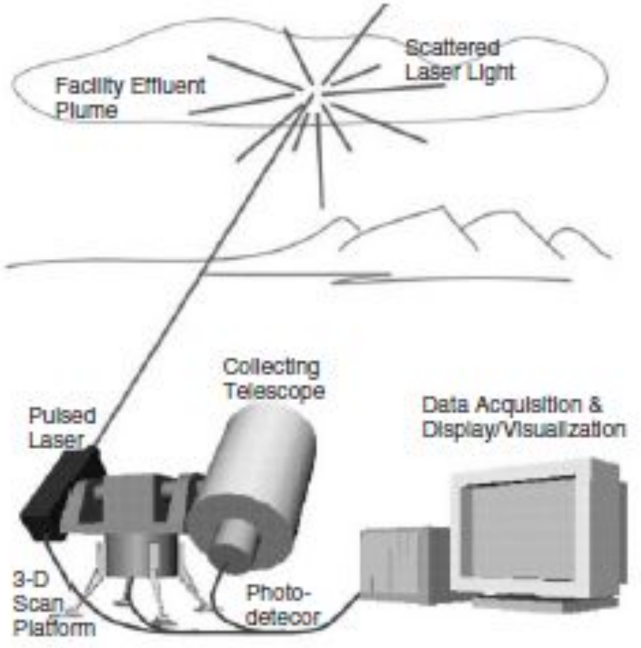

Questions/Comments?

Thank you for listening!

References

Jamie Carter, Keil Schmid, Kirk Waters, Lindy Betzhold, Brian Hadley, Rebecca Mataosky, and Jennifer Halleran, National Oceanic and Atmospheric Administration (NOAA) Coastal Services Center. 2012. "**Lidar 101: An Introduction to Lidar Technology, Data, and Applications**." Revised. Charleston, SC: NOAA Coastal Services Center. https://coast.noaa.gov/data/digitalcoast/pdf/lidar-101.pdf

Comerón A, Muñoz-Porcar C, Rocadenbosch F, Rodríguez-Gómez A, Sicard M. **Current Research in Lidar Technology Used for the Remote Sensing of Atmospheric Aerosols**. *Sensors*. 2017; 17(6):1450. https://doi.org/10.3390/s17061450 .

R. P. Mirin, Senior Member, IEEE, S. W. Nam, Member, IEEE, and M. A. Itzler, Fellow, IEEE **Single-Photon and Photon-Number-Resolving Detectors**, february 15, 2012; accepted February 28, 2012. Date of current version April 20,2012. https://ieeexplore.ieee.org/stamp/stamp.jsp?tp=&arnumber=6251855

Lior Cohen, Elisha S. Matekole, Yoni Sher, Daniel Istrati, Hagai S. Eisenberg, and Jonathan P. Dowling **Thresholded Quantum LIDAR: Exploiting Photon-Number-Resolving Detection** Phys. Rev. Lett. 123, 203601 – Published 11 November 2019 https://journals.aps.org/prl/abstract/10.1103/PhysRevLett.123.203601

G, Altunian, reviewed M, Barton Heine Jr **Signal-to-Noise Ratio and Why It Matters** Home Theater and entertainment Updated on November 11, 2019 https://www.lifewire.com/signal-to-noise-ratio-3134701

Thresholded Quantum LIDAR: Exploiting Photon-Number-Resolving Detection
Lior Cohen ,1,* Elisha S. Matekole,1 Yoni Sher ,2 Daniel Istrati,3 Hagai S. Eisenberg,3 and Jonathan P. Dowling1,4,5,6

Single photon three dimensional imaging at up to 10 kilometers range leonard mw ltm crewe road north edinburgh institute of photonics and quantum sciences, school of engineering and physical sciences

Single-Photon and Photon-Number-Resolving Detectors Volume 4, Number 2, April 2012R. P. Mirin,1 Senior Member, IEEE, S. W. Nam,1 Member, IEEE, and M. A. Itzler,2 Fellow, IEEE

Shallow Bathymetric Mapping via Multistop Single Photoelectron Sensitivity Laser Ranging Kristofer Y. Shrestha, Member, IEEE, William E. Carter,
K. Clint Slatton, Senior Member, IEEE, and Tristan K. Cossio, Member, IEEE

Predicting Small Target Detection Performance of Low-SNR Airborne Lidar Tristan K. Cossio, K. Clint Slatton, Senior Member, IEEE, William E. Carter, Kris Y. Shrestha, Student Member, IEEE, and David Harding

Performance Metrics for Single-Photon Laser Ranging Kristofer Y. Shrestha, Student Member, IEEE, K. Clint Slatton, Senior Member, IEEE, William E. Carter, and Tristan K. Cossio

Improvement of the signal to noise ratio of Lidar echo signal based on wavelet de-noising technique Zhirong Zhou, Dengxin Hua n, Yufeng Wang, Qing Yan, Shichun Li, Yan Li, Hongwei Wang

References

Kovalev, Vladimir A., and William E. Eichinger. **Elastic Lidar: Theory, Practice, and Analysis Methods**. Wiley-Interscience, 2004.

Raman Scattering, Georgia State University, hyperphysics.phy-astr.gsu.edu/hbase/atmos/raman.html.

Yu, Chao, et al. "**Compact and Lightweight 1.5 Mm Lidar with a Multi-Mode Fiber Coupling Free-Running InGaAs/InP Single-Photon Detector.**" Review of Scientific Instruments, vol. 89, no. 10, 2018, p. 103106., doi:10.1063/1.5047472.

Liang Mei, Yichen Li, Zheng Kong, Teng Ma, Zhen Zhang, Ruonan Fei, Yuan Cheng, Zhenfeng Gong, and Kun Liu, "**Mini-Scheimpflug lidar system for all-day atmospheric remote sensing in the boundary layer**," Appl. Opt. 59, 6729-6736 (2020)

Farhani, G., Sica, R. J., and Daley, M. J.: **Classification of lidar measurements using supervised and unsupervised machine learning methods**, Atmos. Meas. Tech., 14, 391–402, https://doi.org/10.5194/amt-14-391-2021, 2021.

Muradyan, P, and R Coulter. **Micropulse Lidar (MPL) Instrument Handbook**. U.S. Department of Energy, Office of Science, Office of Biological and Environmental Research, Mar. 2020, www.arm.gov/publications/tech_reports/handbooks/mpl_handbook.pdf.

"**Differential Absorption Lidar**." *Differential Absorption Lidar - an Overview | ScienceDirect Topics*, www.sciencedirect.com/topics/earth-and-planetary-sciences/differential-absorption-lidar#:~:text=Differential%20absorption%20lidar%20(DIAL)%20is,measurements%20of%20atmospheric%20gas%20concentrations.

Brydegaard, Mikkel, et al. "**The Scheimpflug Lidar Method**." Search the World's Largest Collection of Optics and Photonics Applied Research., International Society for Optics and Photonics, 30 Aug. 2017, www.spiedigitallibrary.org/conference-proceedings-of-spie/10406/2272939/The-Scheimpflug-lidar-method/10.1117/12.2272939.full?SSO=1.